# On working gas rarefaction in high power impulse magnetron sputtering

**K. Barynova[1], S. Suresh Babu[1], M. Rudolph[2], J. Fischer[3], D. Lundin[3], and J. T. Gudmundsson[1,4]**

[1]Science Institute, University of Iceland, Reykjavík, Iceland

[2]Leibniz Institute of Surface Engineering (IOM), Leipzig, Germany

[3]Plasma and Coatings Physics Division, IFM-Materials Physics, Linköping University, Linköping, Sweden

[4]Division of Space and Plasma Physics, KTH Royal Institute of Technology, Stockholm SE-100 44, Sweden

**Abstract**

The ionization region model (IRM) is applied to explore the working gas rarefaction in high power impulse magnetron sputtering discharges operated with graphite, aluminum, copper, titanium, zirconium, and tungsten targets. The various contributions to working gas rarefaction including electron impact ionization, kick-out by the sputtered species, and diffusion, are evaluated and compared for the different target materials, over a range of discharge current densities. For all cases the working gas rarefaction is found to be significant, and to be caused by several processes, and that their relative importance varies between different target materials. In the case of a graphite target, electron impact ionization (primary and secondary electrons) is the dominating contributor to the working gas rarefaction, with 65 – 69% contribution, while the kick-out, or sputter wind, has negligible influence, whereas in the case of tungsten target, the kick-out dominates, with 36 – 43 % contribution. It is not entirely clear what is the main factor determining the relative contribution of the various processes to working gas rarefaction – the mass of the target atom, the ionization potential or the cohesive energy, which determines the most probable velocity with which the sputtered particles leave the target.

## Introduction

Magnetron sputtering is a versatile and widely applied physical vapor deposition technique where the film-forming material is sputtered from a cathode target by ion bombardment [1].

A variation of the magnetron sputtering technique is high power impulse magnetron sputtering (HiPIMS) where the discharge is driven by high power pulses delivered at low repetition frequency, and with low duty cycle [2].

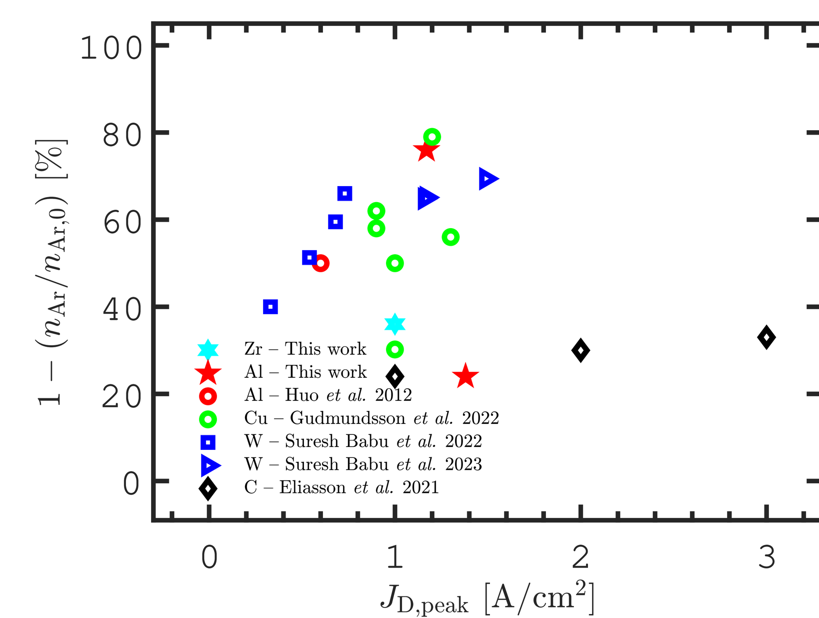


**Figure 1:** The maximum in the degree of working gas rarefaction derived from the IRM versus the peak discharge current density for various target materials.

The sputter process releases the atoms of the film-forming species from the target and the sputtered species enter the discharge with considerable energy, which is determined by the cohesive energy of the solid target.

The interaction between the energetic sputtered particles and the working gas atoms has not only an influence on the momentum of the sputtered species, but also on the discharge properties as it leads to a reduction in the working gas density, or an increase in the working gas temperature, in front of the cathode target [3, 4].

The ionization region model (IRM) is a semi-empirical time-dependent volume averaged plasma chemical model of the ionization region (IR) of the HiPIMS discharge that provides the temporal evolution of the densities of ions, neutrals and electrons with known discharge current and voltage waveforms [5].

Here, using the IRM, we explore the relative contributions of the various terms that contribute to the working gas rarefaction in HiPIMS discharges with a few different target materials, graphite, aluminum, copper, titanium, zirconium, and tungsten.

## Results and discussion

Figure 1 shows the maximum in the degree of working gas rarefaction for a number of discharges with varying target materials modelled in the past, versus the peak discharge current density $J_{\rm D,peak}$.

For the calculation of the degree of working gas rarefaction all neutral argon atoms are taken into account, including the ground state atoms (cold, warm and hot) as well as metastable argon atoms.

It can be seen that in general the degree of working gas rarefaction increases with increased discharge current density, for a given target material.

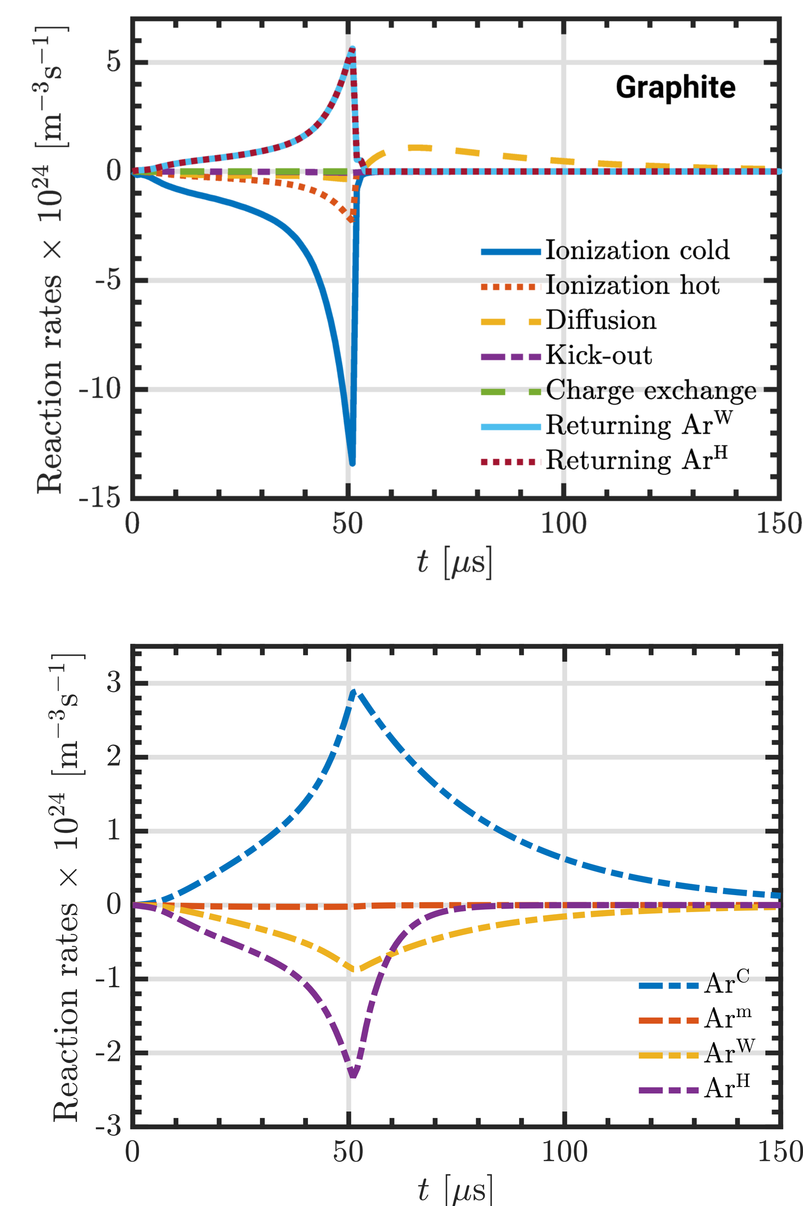


**Figure 2:** (a) The reaction rates for the argon atom loss and gain and (b) the diffusion terms, within the ionization region for a discharge with 50 mm diameter graphite target operated at working gas pressure of 1 Pa, with a peak discharge current $I_{\rm D,peak}$ of 20 A ($J_{\rm D,peak}$ = 1 A/cm$^2$) and 50 $\mu$s long pulse.

Figure 2 shows the temporal evolution of the reaction rates for the loss and gain of argon atoms within the ionization region for a discharge with graphite target and $J_{\rm D,peak} = 1$ A cm$^{-2}$ [6].

The main contributor to the loss of argon atoms is electron impact ionization of the argon atoms by primary electrons, and the second most important loss process is electron impact ionization by secondary electrons.

Warm and hot argon atoms released from the target enter the ionization region and constitute the main contribution to the gain of argon atoms within the ionization region.

The main contribution to the diffusion is the refill of cold argon atoms into the ionization region, while the warm and hot argon atoms escape out of the ionization region, and the hot argon atoms are lost faster than the warm atoms.

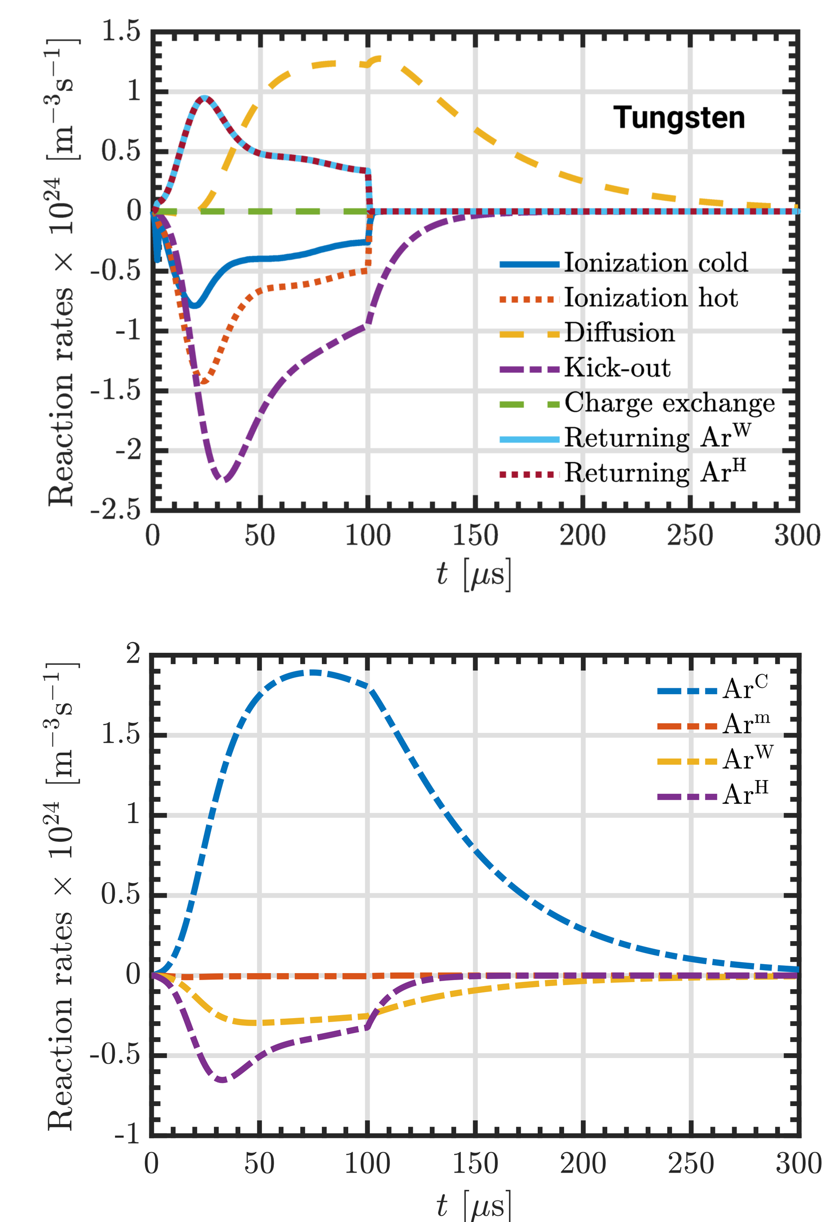


**Figure 3:** (a) The reaction rates for the argon atom loss and gain and (b) the diffusion terms, within the ionization region for a discharge with 75 mm tungsten target operated at working gas pressure of 1 Pa, with a discharge voltage of $V_{\rm D} = 600$ V giving peak discharge current $I_{\rm D,peak}$ of 24 A ($J_{\rm D,peak}$ = 0.54 A/cm$^2$) for 100 $\mu$s long pulse.

Figure 3 shows the reaction rates for the loss and gain of argon atoms within the ionization region for a discharge with tungsten target with $V_{\rm D} = 600$ V ($J_{\rm D,peak} = 0.54$ A cm$^{-3}$) [7].

We see that the main contributor to the loss of argon atoms from the IR is kick-out of the argon atoms by tungsten atoms sputtered from the target. The second most important loss process is electron impact ionization by secondary electrons followed by electron impact ionization by the primary electrons.

Figure 4 shows the various contributions to the rarefaction, versus the atomic mass of the target material for discharges operated at $J_{\rm D,peak} \approx 1$ A/cm$^2$ and working gas pressures $p_{\rm g} \approx 1$ Pa.

The role of electron impact ionization by primary electrons is rather significant for most of the targets explored, but its contribution is smaller for a discharge with copper and tungsten targets, where the kick-out contribution is larger.

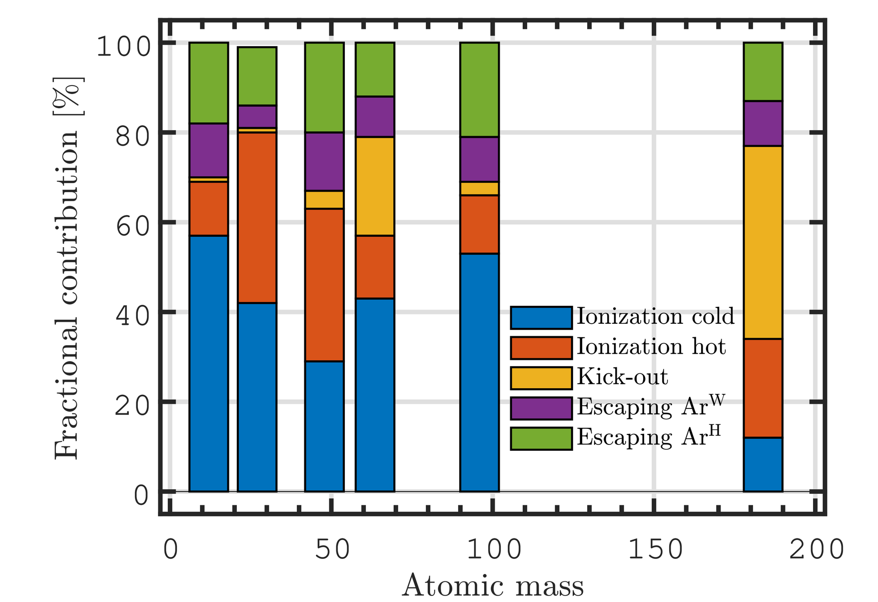


**Figure 4:** The fractional contribution of the various processes to working gas rarefaction within the ionization region versus the atomic mass. The data is for C (12 amu) ($J_{\rm D,peak} = 1$ A/cm$^2$, $t_{\rm pulse} = 50$ $\mu$s, $p_{\rm g} = 1.0$ Pa), Ti (47.9 amu) ($J_{\rm D,peak} = 1.0$ A/cm$^2$, $t_{\rm pulse} = 100$ $\mu$s, $p_{\rm g} = 1.0$ Pa), Cu (63.5 amu) ($J_{\rm D,peak} = 1$ A/cm$^2$, $t_{\rm pulse} = 40$ $\mu$s, $p_{\rm g} = 1.0$ Pa), Al (27.0 amu) ($J_{\rm D,peak} = 1.0$ A/cm$^2$, $t_{\rm pulse} = 100$ $\mu$s, $p_{\rm g} = 0.5$ Pa), Cu (63.5 amu) ($J_{\rm D,peak} = 1$ A/cm$^2$, $t_{\rm pulse} = 40$ $\mu$s, $p_{\rm g} = 1.0$ Pa), Zr (91.2 amu) ($J_{\rm D,peak} = 1$ A/cm$^2$, $t_{\rm pulse} = 50$ $\mu$s, $p_{\rm g} = 1.0$ Pa), and W (183.8 amu) ($J_{\rm D,peak} = 0.73$ A/cm$^2$, $t_{\rm pulse} = 100$ $\mu$s, $p_{\rm g} = 1.0$ Pa).

## Conclusions

We have applied the ionization region model to determine the various contributions to working gas rarefaction in HiPIMS discharges with a number of different cathode targets, spanning a wide range in atomic mass.

The results show that the processes that are responsible for working gas rarefaction and their relative contributions vary greatly depending on the target material.

## References

[1] J. T. Gudmundsson. *Plasma Sources Sci. Technol.*, **29**(11), 113001, 2020.

[2] J. T. Gudmundsson, N. Brenning, D. Lundin, and U. Helmersson. *J. Vac. Sci. Technol. A*, **30**(3), 030801, 2012.

[3] D. W. Hoffman. *J. Vac. Sci. Technol. A*, **3**(3), 561–566, 1985.

[4] S. M. Rossnagel. *J. Vac. Sci. Technol. A*, **6**(1), 19–24, 1988.

[5] Chunqing Huo *et al.* *J. Phys. D: Appl. Phys.*, **50**(35), 354003, 2017.

[6] H. Eliasson *et al.* *Plasma Sources Sci. Technol.*, **30**(11), 115017, 2021.

[7] Swetha Suresh Babu *et al.* *Plasma Sources Sci. Technol.*, **31**(6), 065009, 2022.